

---

# Autoencoding with XCSF

**Richard J. Preen**

richard2.preen@uwe.ac.uk

Department of Computer Science and Creative Technologies  
University of the West of England, Bristol, UK

**Stewart W. Wilson**

wilson@prediction-dynamics.com

Prediction Dynamics, Concord, MA 01742, USA

**Larry Bull**

larry.bull@uwe.ac.uk

Department of Computer Science and Creative Technologies  
University of the West of England, Bristol, UK

---

## Abstract

Autoencoders enable data dimensionality reduction and are a key component of many (deep) learning systems. This article explores the use of the XCSF online evolutionary reinforcement learning system to perform autoencoding. Initial results using a neural network representation and combining artificial evolution with stochastic gradient descent, suggest it is an effective approach to data reduction. The approach adaptively subdivides the input domain into local approximations that are simpler than a global neural network solution. By allowing the number of neurons in the autoencoders to evolve, this further enables the emergence of an ensemble of structurally heterogeneous solutions to cover the problem space. In this case, networks of differing complexity are typically seen to cover different areas of the problem space. Furthermore, the rate of gradient descent applied to each layer is tuned via self-adaptive mutation, thereby reducing the parameter optimisation task.

## Keywords

Autoencoder, evolutionary algorithm, learning classifier system, neural network, self-adaptation, stochastic gradient descent, XCSA, XCSF.

## 1 Introduction

Autoencoders are a core neural network component of many deep learning systems (LeCun et al., 2015) and have significantly contributed to improvements in the current state-of-the-art for speech recognition, object detection, and natural language processing. They may be used simply to perform dimensionality reduction, but can also be combined with a predictive component and further refined under a supervised scheme. Usually, autoencoders are trained using standard neural network backpropagation techniques.

Recently, evolutionary algorithms (EAs) combined in some form with stochastic gradient descent have experienced a resurgence in their use for optimising large neural networks (Stanley et al., 2019). As with the backpropagation techniques, these techniques seek to construct a single large global network that covers the entire feature space. In contrast, the learning classifier system XCSF (Wilson, 2001) provides an EA approach wherein a feature space is adaptively partitioned into niches and local approximations are formed. We suggest that an XCSF-like system might be capable of building an emergent ensemble of heterogeneous autoencoders with possible advantages in performance and efficiency over standard EA techniques.

Following on very initial work with a simple LCS (Bull, 2019), this article adapts XCSF for the autoencoder problem and tests it on numerous datasets. We explore the performance of neural networks with fixed numbers of hidden neurons, as well as allowing their number to evolve, i.e., heterogeneous niched encoders may emerge. Moreover, we introduce a self-adaptive scheme wherein each layer adapts to the local rate of gradient descent applied.

The remainder of this article is organised as follows. Section 2 describes the XCSF learning classifier system, and presents an overview of the related work on neural classifiers and autoencoders. Section 3 describes the neural classifier representation and learning scheme adopted, along with the experimental method applied. Section 4 presents the results from experimentation on a range of publicly available datasets with progressively larger numbers of features. Section 5 presents our conclusions.

## 2 Background

### 2.1 XCSF

XCSF is an accuracy-based online evolutionary reinforcement learning system with locally approximating functions that compute classifier payoff prediction directly from the input state. XCSF can be seen as a generalisation of XCS (Wilson, 1995) where the prediction is a scalar value.

Each XCSF classifier  $cl$  consists of (i) a condition structure  $cl.C$  that determines whether the rule matches input  $\vec{x}$  (ii) an action structure  $cl.A$  that selects an action  $a$  to be performed for a given  $\vec{x}$  (iii) a prediction structure  $cl.P$  that computes the expected payoff for performing  $a$  upon receipt of  $\vec{x}$ . In addition, each classifier maintains a measure of its experience  $exp$ , error  $\epsilon$ , fitness  $F$ , numerosity  $num$ , average participated set size  $s$ , and the time stamp  $ts$  of the last EA invocation on a participating set.

For each learning trial, XCSF constructs a match set  $[M]$  composed of classifiers in the population set  $[P]$  whose  $cl.C$  matches  $\vec{x}$ . If  $[M]$  contains fewer than  $\theta_{\text{mna}}$  actions, a covering mechanism generates classifiers with matching  $cl.C$  and random action  $a$ . For each possible action  $a_k$  in  $[M]$ , XCSF estimates the expected payoff by computing a system prediction  $P(a_k)$ , typically as the fitness-weighted average. That is, for each action  $k$  and classifier prediction  $p_j$  in  $[M]$ , the system prediction  $P_k = \sum_j F_j p_j / \sum_j F_j$ . A system action is then randomly or probabilistically selected during exploration, and the highest payoff action  $P_k$  used during exploitation. Classifiers in  $[M]$  advocating the chosen action are subsequently used to construct an action set  $[A]$ . The action is then performed and a scalar reward  $r \in \mathbb{R}$  received, along with the next sensory input.

In a single-step problem, each classifier  $cl_j \in [A]$  has its experience incremented and fitness, error, and set size updated using the Widrow-Hoff delta rule with learning rate  $\beta \in [0, 1]$  as follows.

$$\triangleright \text{Error: } \epsilon_j \leftarrow \epsilon_j + \beta(|r - p_j| - \epsilon_j)$$

$$\triangleright \text{Accuracy: } \kappa_j = \begin{cases} 1 & \text{if } \epsilon_j < \epsilon_0 \\ \alpha(\epsilon_j/\epsilon_0)^{-\nu} & \text{otherwise.} \end{cases}$$

With target error threshold  $\epsilon_0$  and accuracy fall-off rate  $\alpha \in [0, 1]$ ,  $\nu \in \mathbb{N}_{>0}$ .

$$\triangleright \text{Relative accuracy: } \kappa'_j = (\kappa_j \cdot num_j) / \sum_j \kappa_j \cdot num_j$$

$$\triangleright \text{Fitness: } F_j \leftarrow F_j + \beta(\kappa'_j - F_j)$$

$$\triangleright \text{Set size estimate: } s_j \leftarrow s_j + \beta(|[A]| - s_j)$$

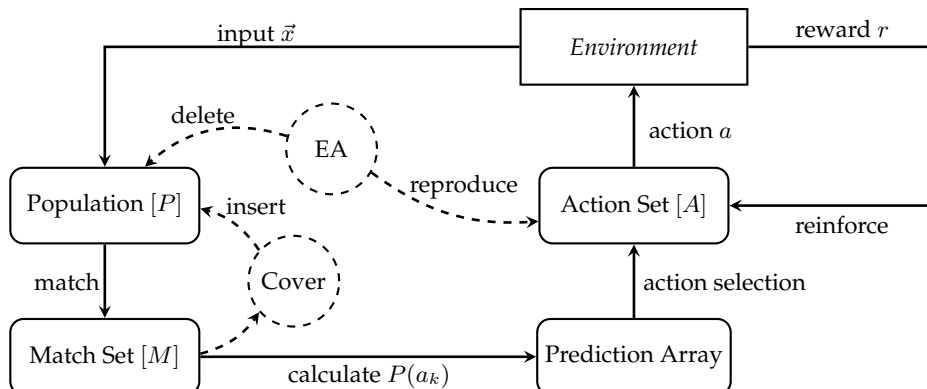


Figure 1: XCSF schematic illustration for single-step classification. In multi-step classification, the EA and reinforcement take place within the previous action set (not shown) using a discounted reward similar to  $Q$ -learning. For regression problems, no action set is necessary; classifier prediction is made directly accessible to the environment, with the EA and reinforcement applied to the match set.

Thereafter,  $cl.C$ ,  $cl.A$ , and  $cl.P$  are updated according to the representation adopted.

The EA is applied to classifiers within  $[A]$  if the average time since its previous execution exceeds  $\theta_{EA}$ . Upon invocation, the  $ts$  of each classifier is updated. Two parents are chosen based on their fitness via roulette wheel selection (or tournament; Butz et al., 2003) and  $\lambda$  number of offspring are created via crossover with probability  $\chi$  and mutation with probability  $\mu$ . Offspring parameters are initialised by setting the error and fitness to the parental average, and discounted by reduction parameters for error  $\epsilon_R$  and fitness  $F_R$ . Offspring  $exp$  and  $num$  are set to one. If subsumption is enabled and the offspring are subsumed by either parent with sufficient accuracy ( $\epsilon_j < \epsilon_0$ ) and experience ( $exp_j > \theta_{sub}$ ), it is not included in  $[P]$ ; instead the parents'  $num$  is incremented. The resulting offspring are added to  $[P]$  and the maximum (micro-classifier) population size  $N$  is enforced by removing classifiers selected via roulette (or tournament) with the deletion vote.

The deletion vote is set proportionally to the set size estimate  $s$ . However, the vote is increased by a factor  $\bar{F}/F_j$  for classifiers that are sufficiently experienced ( $exp_j > \theta_{del}$ ) and with small fitness  $F_j < \delta\bar{F}$ ; where  $\bar{F}$  is the  $[P]$  mean fitness, and typically  $\delta = 0.1$ .

In a multi-step problem, the previous action set  $[A]_{-1}$  is instead updated and the EA may be run therein. For regression problems, no  $[A]$  is necessary and instead  $cl.P$  is made directly accessible to the environment; the EA and reinforcement are performed in  $[M]$ . See schematic illustration in Figure 1.

A number of interacting pressures have been identified within XCS (Butz et al., 2004). A set pressure provides more frequent reproduction opportunities for more general rules. In opposition is a fitness pressure which represses the reproduction of inaccurate and over-general rules. Bernadó-Mansilla and Ho (2005) detail the domain of XCS competence on a range of classification problems, and Orriols-Puig et al. (2009) provide an analysis of XCS for problems with class imbalances. See Bull (2015) for an overview of LCS and Butz (2006) for a detailed introduction to XCSF.

Many forms of  $cl.C$ ,  $cl.A$ , and  $cl.P$  have been used for classifier knowledge since the original ternary conditions, integer actions, and scalar predictions. Notable ex-

amples include, real-valued interval conditions (e.g., Stone and Bull, 2003); symbolic tree conditions (e.g., Iqbal et al., 2014); convex hull conditions (Lanzi and Wilson, 2006); Haar-like feature conditions for image recognition (Ebadi et al., 2014); linear computed predictions (Wilson, 2001), gradient descent predictions (Butz et al., 2005); support vector predictions (Loiacono et al., 2007); Kalman filter predictions (Drugowitsch and Barry, 2008); hyperellipsoidal conditions and recursive least squares predictions (Butz et al., 2008); fuzzy logic (e.g., Casillas et al., 2007); and temporally dynamic graphs (Preen and Bull, 2013). Ensemble approaches have also been considered, both in the homogeneous (Bull et al., 2007), and heterogeneous case (Lanzi et al., 2008).

Perhaps somewhat surprisingly, there had been no previous use of XCS for extracting structure within unlabelled data until the work of Tamee et al. (2007) on clustering, termed XCSC. Clustering is an important unsupervised learning technique where a set of data are grouped into clusters in such a way that data in the same cluster are similar in some sense and data in different clusters are dissimilar in the same sense. They showed how the XCS generalisation mechanisms can be used to identify clusters, both their number and description.

## 2.2 Evolving Neural Classifiers

A long history of searching neural network topologies can be traced back to the origins of computing (Turing, 1948). EAs have been widely used to design single networks, which are typically initialised in a minimal state and their complexity increased; simultaneously adapting the weights and topology (Yao, 1999). Currently, two of the most prevalent methods are NEAT (Stanley and Miikkulainen, 2002) and Cartesian genetic programming (CGP; Khan et al., 2013). Indirect encodings have the potential to scale to very large sized networks (Stanley et al., 2009) and it has been suggested that EAs are competitive with stochastic gradient descent on high-dimensional problems (Morse and Stanley, 2016). Gaier and Ha (2019) have recently shown that evolving the network architecture without explicit weight training can produce similar results to fixed architectures where all weights are adapted.

EAs are able to optimise neural networks even when there is no gradient information available. Moreover, several approaches exist wherein they may be combined with gradient descent techniques. Under a Lamarckian scheme, the learned weights remain as part of the genetic code for evolutionary operators to act upon (Gruau and Whitley, 1993). In contrast, with Baldwinian evolution, lifetime learning is not directly reflected within the genome, but still influences selection (Hinton and Nowlan, 1987).

Following developments in deep learning, there has been a renewed interest in the use of population-based training (Jaderberg et al., 2017) and EAs to design large neural networks (Cui et al., 2018). Concurrently, adaptive gradient descent methods such as AdaGrad, RMSProp, and Adam have become increasingly prevalent. These scale the magnitude of update for each individual parameter based on various moments of the gradient. However, they frequently require some form of annealing (or warm-up schedule) to maintain early stability. These warm-up parameters typically require tuning for a specific problem and model; and the benefits over simple stochastic gradient descent with an appropriate learning rate remain controversial (Wilson et al., 2017).

There has also been a long history of comparison between LCS and neural networks. For example, Smith and Cribbs (1994) compared classifiers with the hidden neurons of a single neural network. Andersen and Tsoi (1993) used an EA with fitness sharing to perform layer-by-layer training of a neural network. In their approach, each individual represents a hidden neuron and the number is allowed to vary within each

layer. Neurons are partitioned into sets that perform similar functions and a representative from each set is chosen to form the layer. Layers are added after a fixed number of search generations. Fitness sharing encourages the formation of different feature detectors (hidden neurons) within the population.

Bull (2002) was the first to represent LCS classifiers as neural networks: both *cl.C* and *cl.A* were performed within a single network rule. Subsequently, self-adaptive mutation was applied (Bull and Hurst, 2003), as was stochastic gradient descent (O’Hara and Bull, 2005b). In the latter approach, local search was performed by adapting the weights of the least fit networks in  $[A]$  towards the fittest rule in the set.

O’Hara and Bull (2007) also used neural classifiers for function approximation where gradient descent was used to update the *cl.P* weights using the target outputs—there single networks performed *cl.C* and *cl.P*. With the inclusion of an additional classifier network to predict the next state input, O’Hara and Bull (2005a) extended the approach for anticipatory LCS. More recently, Howard et al. (2016) have explored the more biologically plausible spiking neural networks within LCS, adapting both the number of neurons and connections to perform temporal reinforcement learning.

Neural networks have also been paired with other classifier representations within LCS. For example, Lanzi and Loiacono (2006) used hyperrectangle *cl.C* and neural network *cl.P* within XCSF. There, the EA adapted the network topology but not the weights. The weights were updated using the XCSF version of the delta rule (Wilson, 2002) to compute the expected payoff. Dam et al. (2008) also explored hyperrectangle *cl.C* and neural network *cl.A* within UCS. In addition, Sancho-Asensio et al. (2014) presented a neural LCS for data stream classification. Recently, Kim and Cho (2019) have investigated an LCS where the EA performs feature selection using bitstring conditions and a selection of convolutional neural network actions are used.

### 2.3 Autoencoding

Autoencoders are composed of an encoder and decoder, which are jointly trained to minimise the discrepancy between the original input data and its reconstruction. To capture useful structure, the encoder must be prevented from simply learning an identity function. Typically this is achieved by constraining the size of the encoder. However, regularisation techniques are also effective. For example, the use of sparsity (Ranzato et al., 2007) and contractive (Rifai et al., 2011) constraints, the addition of noise (Vincent et al., 2010), and signal dropout of neurons (Srivastava et al., 2014) or weights (Wan et al., 2013).

After pretraining the feature detector layers, they can be combined with a predictive layer for classification or regression, and further refined under a supervised scheme. Figure 2 illustrates the general architecture. Deep autoencoders can be formed by stacking multiple single-layer autoencoders and using greedy layerwise unsupervised training (Hinton and Salakhutdinov, 2006). They may also be placed in a recursive configuration (Socher et al., 2011).

Erhan et al. (2010) have shown two key reasons why the unsupervised pretraining of neural network feature detectors significantly improves subsequent supervised learning with stochastic gradient descent (Rumelhart et al., 1986). The first is that it makes the optimisation task easier because the weights are initialised in an appropriate region of the space. The second benefit is that generalisation on test data is significantly improved because the learned weights originate from modelling input patterns rather than the function mapping input to label. This becomes of even greater importance where there is a large amount of unlabelled data available for pretraining and

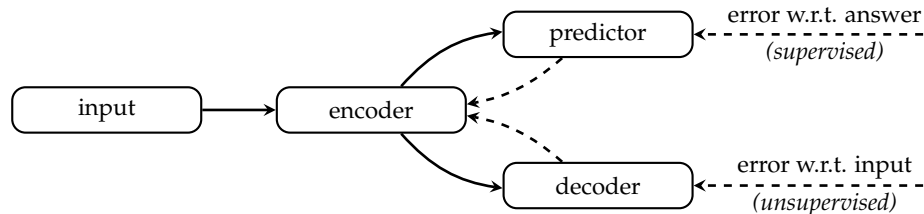


Figure 2: Autoencoder architecture. In the first phase, the encoder-decoder is trained to reconstruct the original inputs. Thereafter, the encoder may be paired with a predictor and further trained to minimise the error with respect to labelled instances.

only a relatively small amount of labelled data for predictive training. Moreover, autoencoders can be used for a wide number of tasks even without any labelled data. For example, imputing missing data values (Abdella and Marwala, 2005) and anomaly detection (Sakurada and Yairi, 2014).

EAs have frequently been used to design autoencoders. For example, Fernando et al. (2016) used an EA to design the topology of compositional pattern producing networks (CPPNs) where the outputs were taken as the weights of a neural network autoencoder. The autoencoder was subsequently refined via gradient descent and the resulting gradients used to update the CPPN weights. Sun et al. (2019) used an EA to evolve deep neural networks for feature learning via an unsupervised scheme. See Bengio et al. (2013) for a general overview of feature learning and autoencoding, and Xue et al. (2016) for evolutionary computing approaches to feature selection.

Autoencoding via a single neural network has recently been used with XCS (Matsumoto et al., 2017). The feature inputs were initially passed through a pretrained encoder to reduce the dimensionality before performing XCS classification with an interval encoding.

Historically, somewhat akin to autoencoding, Booker (1988) presented a form of LCS which extends the principle of using an EA to discover any underlying regularities in the problem space, dividing the task of learning such structure from that of supplying appropriate actions to receive external reward. A separate LCS exists for each of these two aspects. A first LCS receives binary encoded descriptions of the external environment, with the objective to learn appropriate regularities through generalisations over the input space. This is seen as analogous to learning to represent categories of objects. The matching rules not only post their actions/outputs onto their own internal memory/message list but some are passed as inputs to a second LCS. The second LCS receives reward when it correctly exploits such categorisations with respect to the current task. See (Bull and Fogarty, 1994) for a related LCS using only an EA.

### 3 Methodology

Here, we use a derivative of XCSF to explore the autoencoding of multi-layer perceptron neural networks—a system herein termed XCSA. That is, each classifier is trained to reproduce its inputs via a much smaller (encoding) hidden layer. Each  $cl.C$  and  $cl.P$  is a separate fully-connected neural network, as illustrated in Figure 3. Each network is composed of hidden rectified linear units (He et al., 2015), and logistic outputs. The  $cl.C$  output layer contains a single neuron that determines whether the rule matches a given input. The  $cl.P$  (decoding) output layer contains as many output neurons as

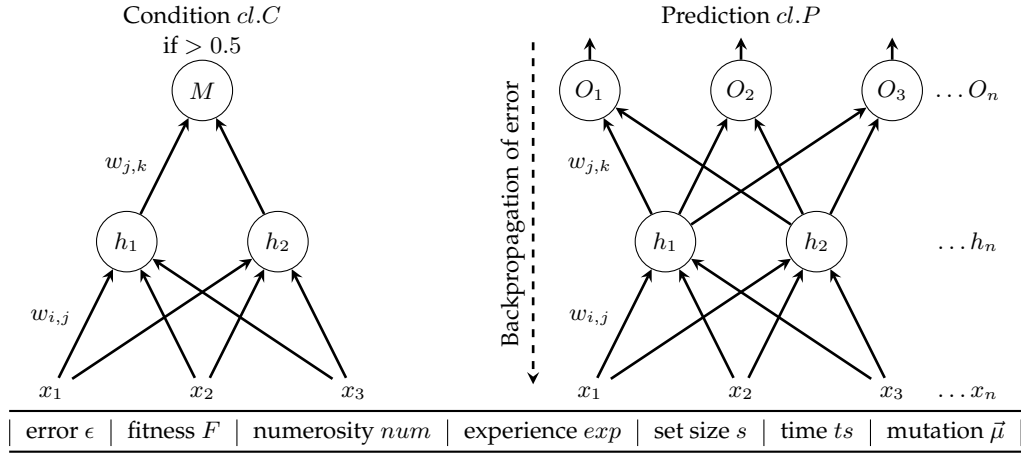


Figure 3: Neural classifier knowledge representation. Separate fully-connected feed-forward networks calculate classifier matching and prediction. Each layer is encoded as a vector of weights (and biases), along with an activation function and gradient descent rate. Evolutionary operators are applied to the weights and topology of both  $cl.C$  and  $cl.P$  upon reproduction using the self-adaptive mutation rates.

inputs.

A population of  $N = 1000$  classifiers are initialised randomly and undertake Lamarckian learning. That is, after the application of evolutionary operators to both  $cl.C$  and  $cl.P$  during reproduction, stochastic gradient descent updates  $cl.P$  during reinforcement. The resulting  $cl.P$  weights are copied to offspring upon parental selection.

During instantiation of  $[P]$  the weights of each network are initialised with small random values sampled from a Gaussian normal distribution with mean  $m = 0$  and standard deviation  $\sigma = 0.1$ . Biases are zero initialised. Should covering be triggered at any stage, networks with random weights and biases are generated by the same method until the network matches the current input, however using a larger  $\sigma = 1$ . Upon receipt of  $\vec{x}$ ,  $[M]$  is formed by adding all  $cl \in [P]$  whose  $cl.C$  outputs a value greater than 0.5.

Classifier reinforcement and the EA take place within  $[M]$ . The  $[M]$  fitness-weighted average prediction is also used for system output as usual in XCSF. However, learning in XCSA consists of updating the matching error, which is derived from the mean squared error (MSE) with respect to  $\vec{x}$  and the corresponding values on each output neuron  $O$  of a rule in the current  $[M]$  using the modified Widrow-Hoff delta rule with learning rate  $\beta$ :

$$\epsilon_j \leftarrow \epsilon_j + \beta \left[ \frac{1}{n} \sum_{i=1}^n (x_i - O_i)^2 - \epsilon_j \right] \quad (1)$$

Subsequently, each  $cl.P$  within  $[M]$  is updated using simple stochastic gradient descent (Rumelhart et al., 1986) with learning rate  $\eta \in \mathbb{R}_{>0}$  and momentum  $\omega \in [0, 1]$ . That is, the chain rule is applied at match time  $t$  to compute the partial derivative of the error with respect to each weight  $\partial\mathcal{E}/\partial w$ , and the weight change:

$$\Delta w_t = -\eta \partial\mathcal{E}/\partial w_t + \omega \Delta w_{t-1} \quad (2)$$

Gradient descent is not applied to  $cl.C$ .

Following (Bull and Hurst, 2003) crossover is omitted and self-adaptive mutation used. Each classifier maintains a vector of mutation rates initially seeded randomly from a uniform distribution  $\vec{\mu} \sim U[\mu_{\min}, 1]$ . These parameters are passed to its offspring. The offspring then applies each of these mutation rates to itself using a Gaussian distribution, i.e.,  $\mu'_i = \mu_i e^{\mathcal{N}(0,1)}$ , before mutating the rest of the rule at the resulting rate. This is similar to the approach used in evolution strategies (ES; Schwefel, 1981) where the mutation rate is a locally evolving entity in itself, i.e., it adapts during the search process. Self-adaptive mutation not only reduces the number of hand-tunable parameters of the EA, it has also been shown to improve performance. Here, three types of mutation are explored:

- Weights and biases are adapted through the use of a single self-adaptive mutation rate, which controls the  $\sigma$  of a random Gaussian added to each weight and bias. This is also similar to the approach used in ES.
- The topology is adapted through the use of a second self-adaptive rate, which controls the probability of modifying the number of hidden neurons in the conditions  $C_h$  and predictions  $P_h$ . When triggered, a single hidden neuron is added or the most recently added neuron removed with equal chance. Pressure to evolve minimally sized networks is achieved by altering the population size enforcement mechanism as follows. Each time a classifier must be removed, two classifiers are selected via roulette wheel with the deletion vote as described above and then the rule with the most hidden layer nodes is deleted.
- To adapt the rate of gradient descent, each layer maintains its own  $\eta$ . These values are constrained  $[10^{-4}, 0.1]$  and seeded uniformly random. A third self-adaptive mutation rate controls the  $\sigma$  of a random Gaussian added to each  $\eta$ , similar to weight adaptation. Wyatt and Bull (2005) have previously shown how the self-adaptation of local search parameters can speed learning within XCS.

For baseline comparison, an EA is run by using a population with  $cl.C$  that always match  $\vec{x}$  and the minimum number of hidden neurons required to achieve an error below  $\epsilon_0 = 0.01$  is shown. That is, single networks that cover the entire state-space are learned. For each dataset, the performance of XCSA is shown with fixed numbers of hidden neurons in  $cl.C$  and  $cl.P$ . Additionally, the XCSA learning performance is shown where the number of hidden neurons are evolved; starting with a single hidden neuron in each network ( $h_I = 1$ ) and where the number of hidden neurons are initialised randomly (with 1 fewer than the number of inputs as maximum;  $h_I = R$ ).

Inputs are scaled  $[0, 1]$  and instances are drawn at random. 90% of the sample instances are used for training and 10% reserved for validation. The MSE is used as XCSA loss function. Ten runs for each experiment are performed to 100,000 trials. All graphs presented depict mean  $[P]$  values. Each experiment is performed with  $\eta = 0.01$  (shown graphically) and  $\eta = 0.001$  (not shown). The MNIST dataset is used to demonstrate learning performance where the gradient descent rates are evolved ( $\eta = \text{evo}$ ). Table 1 lists the parameters used.

The following publicly available datasets are used for initial evaluation:

1. UCI vowel dataset: speech recognition; 12 features; 11 classes; 990 instances. Available from <https://www.openml.org/d/307>.
2. UCI thyroid-allbp dataset: classification; 26 features; 5 classes; 2,800 instances. Available from <https://www.openml.org/d/40474>.



Table 1: XCSA and stochastic gradient descent learning parameters used

Description	Parameter	Value
Maximum population size (in micro-classifiers)	$N$	1000
Population initialised with random classifiers	$P_{\text{init}}$	true
Target error	$\epsilon_0$	0.01
Classifier fitness fall-off rate (1=disabled)	$\alpha$	1
Update rate for classifier fitness, error, and set size	$\beta$	0.1
Fraction of (least fit) classifiers to increase deletion vote	$\delta$	0.1
Fitness exponent	$\nu$	5
Classifier deletion threshold	$\theta_{\text{del}}$	20
Classifier initial fitness	$F_I$	0.01
Classifier initial error	$\epsilon_I$	0
Offspring fitness reduction (1=disabled)	$F_R$	0.1
Offspring error reduction (1=disabled)	$\epsilon_R$	1
Minimum number of actions in $[M]$	$\theta_{\text{mna}}$	1
EA invocation frequency	$\theta_{\text{EA}}$	50
Number of offspring per EA invocation	$\lambda$	2
Crossover probability	$\chi$	0
Minimum self-adaptive mutation value	$\mu_{\text{min}}$	0.01
Stochastic gradient descent learning rate	$\eta$	0.01
Stochastic gradient descent momentum	$\omega$	0.9
Initial number of hidden neurons (when evolved)	$h_I$	$\{1, R\}$
Whether EA subsumption is performed	<i>doEASubsume</i>	false
Whether set subsumption is performed	<i>doSetSubsume</i>	false

3. UCI plant leaf (texture) dataset: classification; 64 features; 10 classes; 1,599 instances. Available from <https://www.openml.org/d/1493>.
4. UCI Nomao dataset: classification; 118 features; 2 classes; 34,465 instances. Available from <https://www.openml.org/d/1486>.
5. USPS dataset: image classification; 256 features; 10 classes; 9,298 instances. Available from <https://www.openml.org/d/41082>.
6. MNIST dataset: image classification; 784 features; 10 classes; 70,000 instances. Available from <https://www.openml.org/d/554>.

When comparing experiments on a single dataset, we use the Wilcoxon ranked-sums test, with the null hypothesis that all observed results come from the same distribution. To compare the performance of learning rates across datasets, we follow the recommendations of Demšar (2006) and apply a Wilcoxon signed ranks test on the mean errors (after 100,000 trials) for each experiment, grouped by learning rate.

## 4 Results

### 4.1 UCI vowel dataset

The traditional EA approach requires at least 5 hidden neurons to achieve an autoencoding error below  $\epsilon_0$ . In contrast, XCSA requires  $P_h \geq 3$ . Evolving the number of hidden neurons with  $h_I = 1$  results in  $C_h = 1.22$  and  $P_h = 2.2$  after 100,000 trials.

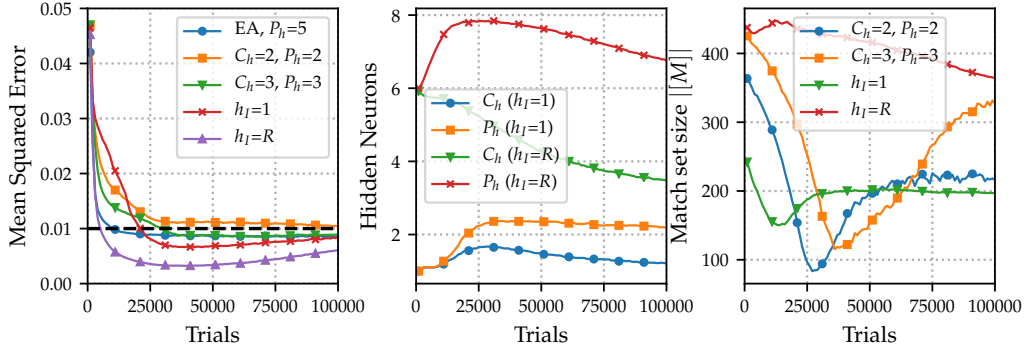


Figure 4: UCI vowel dataset autoencoding of a single hidden layer.

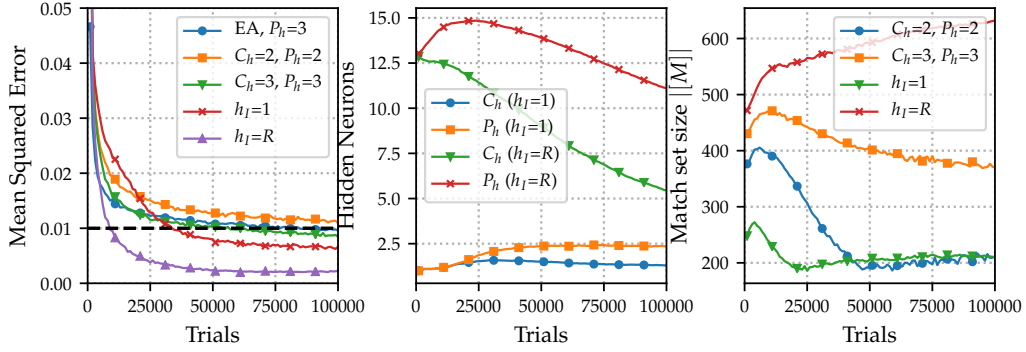


Figure 5: UCI thyroid-allbp dataset autoencoding of a single hidden layer.

In comparison,  $C_h = 3.49$  and  $P_h = 6.76$  when starting with  $h_I = R$ . The hidden neurons in both experiments were still declining at the end of the runs. Increasing the number of hidden neurons from 2 to 3 increases classifier generalisation capability, which is reflected by the larger average match set size  $|M|$ : 217 compared with 317 after 100,000 trials. This effect is also observed when evolving the number of neurons, with  $|M| = 197$  for  $h_I = 1$ , compared with 364 when  $h_I = R$ . The training error for  $h_I = R$  is significantly smaller than  $h_I = 1$  ( $p \leq .01$ ), however there is no difference in validation error. See Figure 4.

#### 4.2 UCI thyroid-allbp dataset

Similar results are observed on the UCI thyroid-allbp dataset, although here slightly fewer hidden neurons are needed despite the additional number of features. The EA requires at least 3 hidden neurons to reach  $\epsilon_0$ . Evolving the number of hidden neurons with  $h_I = 1$  results in  $C_h = 1.29$  and  $P_h = 2.35$  after 100,000 trials, compared with  $C_h = 5.46$  and  $P_h = 11.11$  for  $h_I = R$ . The training and validation errors for  $h_I = R$  are both significantly smaller than  $h_I = 1$ ;  $p \leq .01$ . See Figure 5.

#### 4.3 UCI plant leaf dataset

At least 3 hidden neurons are required to achieve an autoencoding error smaller than  $\epsilon_0$  for the EA on the UCI plant leaf dataset. XCSA reaches the target error with  $C_h = 1$  and  $P_h = 2$ . Evolving the number of hidden neurons with  $h_I = 1$  results in  $C_h = 1.27$  and

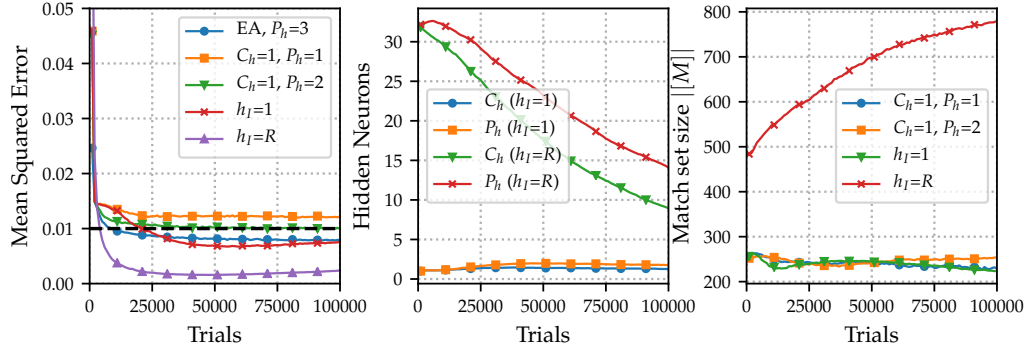


Figure 6: UCI plant leaf dataset autoencoding of a single hidden layer.

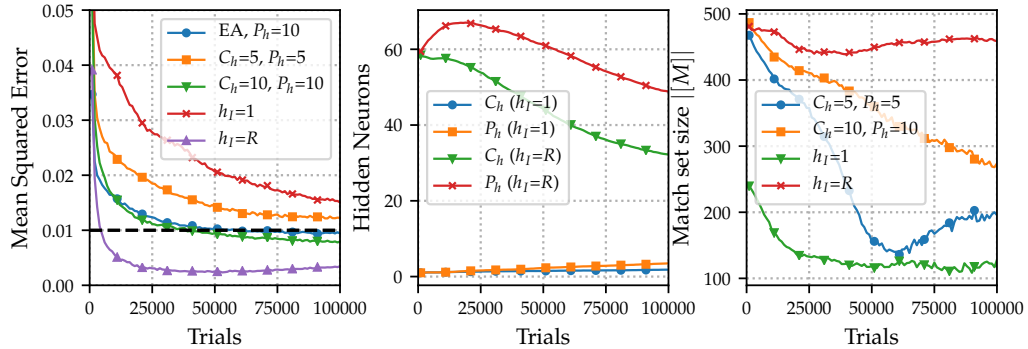


Figure 7: UCI Nomao dataset autoencoding of a single hidden layer.

$P_h = 1.77$  after 100,000 trials. Evolving the number of hidden neurons with  $h_I = R$  results in a significantly smaller training and validation error than  $h_I = 1$ ;  $p \leq .01$ . However, the number of hidden neurons remains much larger:  $C_h = 8.95$  and  $P_h = 14.09$ . On average, there is a reduction in the number of hidden neurons of around two thirds their original number for  $cl.C$  and around half for  $cl.P$  after 100,000 trials. Both were still declining at the end of the runs. Furthermore, the training and validation errors are significantly smaller when comparing  $h_I = 1$  with a similar fixed topology of  $C_h = 1$  and  $P_h = 2$ ;  $p \leq .01$ . See Figure 6.

#### 4.4 UCI Nomao dataset

On the UCI Nomao dataset the EA requires at least 10 hidden neurons. After 100,000 trials, evolving the number of neurons with  $h_I = 1$  reaches an average  $C_h = 1.81$  and  $P_h = 3.49$  with training MSE =  $0.0151 \pm 0.0016$ . Evolving with  $h_I = R$ , rapidly achieves a training error below  $\epsilon_0$ , with  $C_h = 32.21$  and  $P_h = 48.83$  after 100,000 trials. This is a reduction of around half of the original number of  $cl.C$  hidden neurons, on average. Furthermore, the validation MSE =  $0.0068 \pm 0.0004$ , showing that there has been no overfitting of the data. See Figure 7.

#### 4.5 USPS dataset

At least 20 hidden neurons are required by the EA and more than  $P_h = 10$  by XCSA to reach  $\epsilon_0$  on the USPS dataset. After 100,000 trials, evolving the number of neurons

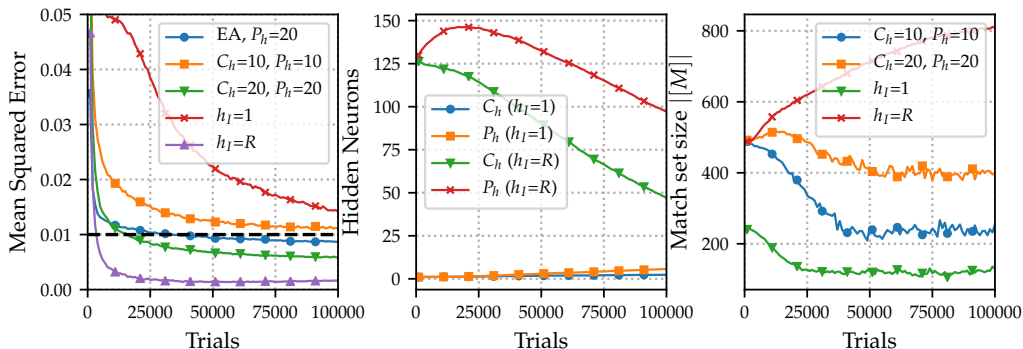


Figure 8: USPS dataset autoencoding of a single hidden layer.

with  $h_I = 1$  reaches an average  $C_h = 2.35$  and  $P_h = 5.7$  with training  $\text{MSE} = 0.0143 \pm 0.0019$ . From Figure 8, it can be seen that the error remains in decline at the end of the experiment, while the number of hidden neurons continues to grow. The target error may therefore be expected to be reached within an additional 100,000 trials given the rate of neuron growth. When  $h_I = R$ , over 75 *cl.C* hidden neurons and 25 *cl.P* hidden neurons are removed on average over the course of the experiment, without any increase in training error. Moreover, the validation  $\text{MSE}$  ( $0.0019 \pm 0.0001$ ) is significantly lower than all of the other experiments, showing that it has not overfit the data;  $p \leq .01$ . However, the computational cost is far greater given the additional neurons. Following the general pattern observed over the previous datasets, the average  $|[M]|$  is correlated with  $P_h$ , as one might expect from additional generalisation power.

#### 4.6 MNIST dataset

On the MNIST dataset, the maximum initial number of hidden neurons for  $h_I = R$  is set to half the number of inputs due to the extra computational cost. From Figure 9 it can be seen that both the EA and XCSA with fixed numbers of hidden neurons are unable to reach  $\epsilon_0$  with  $\eta = 0.01$ . However, the target error can be reached with  $P_h \geq 40$  when using a smaller gradient descent rate  $\eta = 0.001$ . For example, after 100,000 trials, the EA with  $P_h = 40$  and  $\eta = 0.01$  has a significantly larger training and validation  $\text{MSE}$  ( $0.029 \pm 0.0016$ ) when compared with  $\eta = 0.001$  ( $\text{MSE} = 0.009 \pm 0.0001$ );  $p \leq .01$ .

After 100,000 trials, evolving the number of neurons with  $h_I = 1$  and  $\eta = 0.001$  reaches an average  $C_h = 1.58$  and  $P_h = 4.42$  with training  $\text{MSE} = 0.0285 \pm 0.0019$ . The number of neurons are similar to USPS, suggesting that the maximum rate of hidden neuron growth is  $\approx 1$  every 25,000 trials on average. Given that  $P_h \approx 40$  are needed, a rough estimate of around 1 million trials would need to be performed to reach  $\epsilon_0$  when starting from a single hidden neuron. This highlights that while evolution can effectively adapt the number of hidden neurons, it remains important to seed the networks with a suitable initial number. With  $h_I = R$  and  $\eta = 0.001$ , after 100,000 trials  $C_h = 97.63$  and  $P_h = 182.54$  with training  $\text{MSE} = 0.0023 \pm 0.0001$ . This is a reduction of almost 100 *cl.C* hidden neurons on average. Furthermore, the validation  $\text{MSE}$  ( $0.0023 \pm 0.0001$ ) is smaller than  $\epsilon_0$ , showing that it has not overfit the data.

Figure 10 shows the learning performance where each layer also maintains its own  $\eta$ , which is evolved via self-adaptive mutation. As can be seen, the gradient descent rates are suitably adapted to the task and the performance of the EA and XCSA are both similar to  $\eta = 0.001$ . Excluding the case where  $h_I = 1$ , the EA and XCSA have

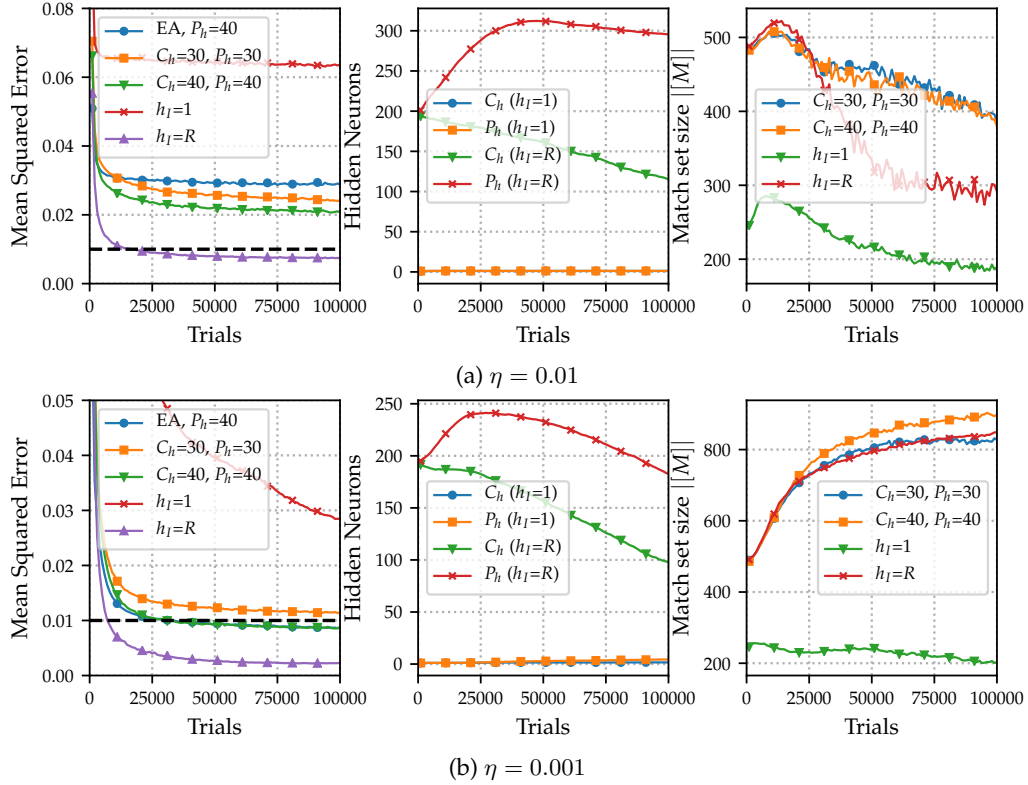


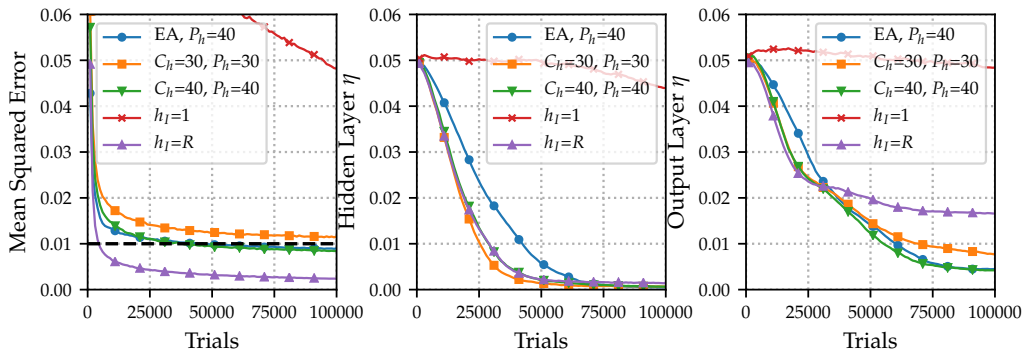
Figure 9: MNIST dataset autoencoding of a single hidden layer.

significantly smaller validation errors than  $\eta = 0.01$ , and there is no significant difference when compared with  $\eta = 0.001$ ;  $p \leq .01$ . Starting with a single hidden neuron on the MNIST dataset is clearly problematic and the self-adaptive rates are unable to work effectively: the validation error is significantly greater than  $\eta = 0.001$ ;  $p \leq .01$ . However, since it can be seen that there are small downward slopes in the MSE and  $\eta$  values, it is possible that suitable values would be identified with a larger population size and number of learning trials.

#### 4.7 Summary

For each dataset, it has been shown that XCSA can effectively train an ensemble of autoencoders to reach the target error by adapting the weights of appropriately sized networks. In addition, it has been shown that XCSA can discover the topologies by allowing the number of hidden neurons to adapt. In each case, the number of hidden neurons can be seen to grow or shrink as appropriate for the task. Moreover, it was shown how self-adaptive gradient descent can be included to automatically identify the appropriate rate of local search to perform.

Two fixed gradient descent learning rates were tested for each experiment on each dataset:  $\eta = 0.01$  and  $0.001$ . With the exception of MNIST, the two gradient descent rates result in similar performance, although with a slower decline in MSE for the smaller  $\eta$ . A Wilcoxon signed ranks test finds that this performance is significantly different, with  $\eta = 0.01$  having smaller training and validation error after 100,000 trials;

Figure 10: MNIST dataset with self-adaptive gradient descent in each layer ( $\eta = \text{evo}$ ).

$p \leq .01$ . On the MNIST dataset however, a smaller  $\eta$  was found to significantly improve performance. By providing each layer with its own evolved  $\eta$ , an adaptive gradient descent was shown capable of automatically determining the appropriate rate.

A summary of the results after 100,000 trials for each of the experiments evolving the number of hidden neurons is shown in Table 2. To see if the potential for heterogeneity over the problem space is beneficial, experiments using the closest-size discovered networks were also run for the UCI datasets. That is, for  $h_I = 1$ , the resulting  $C_h$  and  $P_h$  were rounded to the nearest whole numbers after 100,000 trials and the experiments rerun. In each case,  $h_I = 1$  has a significantly smaller training error;  $p \leq .01$ . This difference in performance shows that XCSA is making use of heterogeneous solutions and the resulting performance is never worse than if the parameters had been found through trial and error. Such an ensemble of heterogeneous autoencoders can be seen to share characteristics with single network sparse autoencoders (e.g., Zeng et al., 2018).

XCSA directly allocates reward to the sub-solutions. Whereas with the EA, the individual being rewarded (or reinforced) represents the overall solution to the problem, and credit is therefore much less direct in terms of rewarding the components actually responsible for the decision. XCSA is also computationally more efficient per trial since reinforcement (including gradient descent) is only applied to  $cl.P$  within  $[M]$  whereas the EA updates all classifiers in  $[P]$ .

## 5 Conclusion

Autoencoding is a key component of many deep learning systems and this article has presented results from using a variant of XCSF to perform such dimensionality reduction. Moreover, given their basis in EAs, LCS do not require the existence of helpful gradients within the weight space, although gradient-based search can speed learning, as here.

The LCS approach adaptively subdivides the input domain into local approximations that are much simpler than a global neural network solution. This further enables the emergence of an ensemble of structurally heterogeneous solutions to cover the problem space. In this case, when the number of neurons in the autoencoders is allowed to evolve, networks of differing complexity are typically seen to cover different areas of the problem space. Additionally, the scheme introduced here entirely self-adapts the search process: both the gradient-free mutation of weights and their local

Table 2: Summary of autoencoding runs after 100,000 trials when evolving the number of hidden neurons; starting with a single neuron  $h_I = 1$  and a random number  $h_I = R$ . Shown are the  $[P]$  mean number of hidden neurons in the conditions  $C_h$  and predictions  $P_h$ , the mean match set size  $||[M]||$ , and the mean error  $\pm$  standard error.

Dataset	$\eta$	$h_I$	$C_h$	$P_h$	$  [M]  $	Training MSE	Validation MSE
Vowel	0.010	1	1.22	2.20	197	$0.0083 \pm 0.0002$	$0.0166 \pm 0.0007$
Vowel	0.001	1	1.36	2.32	175	$0.0089 \pm 0.0015$	$0.0163 \pm 0.0019$
Vowel	0.010	$R$	3.49	6.76	364	$0.0061 \pm 0.0002$	$0.0148 \pm 0.0008$
Vowel	0.001	$R$	3.78	8.00	485	$0.0044 \pm 0.0002$	$0.0137 \pm 0.0012$
Thyroid	0.010	1	1.29	3.35	210	$0.0066 \pm 0.0006$	$0.0195 \pm 0.0006$
Thyroid	0.001	1	1.50	2.35	178	$0.0118 \pm 0.0011$	$0.0249 \pm 0.0013$
Thyroid	0.010	$R$	5.46	11.11	632	$0.0022 \pm 0.0006$	$0.0136 \pm 0.0009$
Thyroid	0.001	$R$	7.80	17.33	716	$0.0044 \pm 0.0001$	$0.0147 \pm 0.0018$
Plant	0.010	1	1.27	1.77	224	$0.0075 \pm 0.0002$	$0.0174 \pm 0.0005$
Plant	0.001	1	1.21	1.45	205	$0.0122 \pm 0.0009$	$0.0253 \pm 0.0017$
Plant	0.010	$R$	8.95	14.09	780	$0.0024 \pm 0.0001$	$0.0066 \pm 0.0004$
Plant	0.001	$R$	12.85	24.88	789	$0.0031 \pm 0.0001$	$0.0078 \pm 0.0001$
Nomao	0.010	1	1.81	3.49	128	$0.0151 \pm 0.0016$	$0.0198 \pm 0.0020$
Nomao	0.001	1	1.51	3.13	159	$0.0123 \pm 0.0011$	$0.0178 \pm 0.0019$
Nomao	0.010	$R$	32.21	48.83	459	$0.0034 \pm 0.0001$	$0.0068 \pm 0.0004$
Nomao	0.001	$R$	32.67	45.40	458	$0.0035 \pm 0.0003$	$0.0092 \pm 0.0012$
USPS	0.010	1	2.35	5.70	130	$0.0143 \pm 0.0019$	$0.0121 \pm 0.0013$
USPS	0.001	1	1.65	4.41	174	$0.0126 \pm 0.0010$	$0.0130 \pm 0.0009$
USPS	0.010	$R$	47.11	97.24	809	$0.0016 \pm 0.0001$	$0.0019 \pm 0.0001$
USPS	0.001	$R$	61.95	87.42	808	$0.0018 \pm 0.0001$	$0.0021 \pm 0.0002$
MNIST	0.010	1	1.25	1.23	189	$0.0636 \pm 0.0002$	$0.0635 \pm 0.0002$
MNIST	0.001	1	1.58	4.42	203	$0.0285 \pm 0.0019$	$0.0284 \pm 0.0019$
MNIST	evol.	1	1.45	2.04	174	$0.0482 \pm 0.0044$	$0.0479 \pm 0.0043$
MNIST	0.010	$R$	115.72	295.72	292	$0.0074 \pm 0.0002$	$0.0078 \pm 0.0002$
MNIST	0.001	$R$	97.63	182.54	849	$0.0023 \pm 0.0001$	$0.0023 \pm 0.0001$
MNIST	evol.	$R$	165.22	264.53	884	$0.0024 \pm 0.0001$	$0.0025 \pm 0.0001$

refinement where gradient information is available. Not only does this potentially reduce the number of hand-tuneable parameters in deep learning, it may provide further benefits in network analysis, use in non-stationary and online domains, etc. Furthermore, the LCS ensemble may reveal input categories more clearly than are seen in a global network solution.

Current work is exploring additional layers of autoencoding, as well as a final classification LCS to determine the effectiveness of the suggested dimensionality reduction shown here on various data sets.

## References

- Abdella, M. and Marwala, T. (2005). The use of genetic algorithms and neural networks to approximate missing data in database. In Rudas, I. J., editor, *Proceedings of the IEEE International Conference on Computational Cybernetics*, pages 207–212. Piscataway, NJ, USA: IEEE Press.
- Andersen, H. C. and Tsoi, A. C. (1993). A constructive algorithm for the training of a multilayer perceptron based on the genetic algorithm. *Complex Systems*, 7(4):249–268.

- Bengio, Y., Courville, A., and Vincent, P. (2013). Representation learning: A review and new perspectives. *IEEE Transactions on Pattern Analysis and Machine Intelligence*, 35(8):1798–1828.
- Bernadó-Mansilla, E. and Ho, T. K. (2005). Domain of competence of XCS classifier system in complexity measurement space. *IEEE Transactions on Evolutionary Computation*, 9(1):82–104.
- Booker, L. B. (1988). Classifier systems that learn internal world models. *Machine Learning*, 3(2–3):161–192.
- Bull, L. (2002). On using constructivism in neural classifier systems. In Guervós, J. J. M. et al., editors, *Parallel Problem Solving from Nature – PPSN VII*, volume 2439 of LNCS, pages 558–567. Berlin, Germany: Springer-Verlag.
- Bull, L. (2015). A brief history of learning classifier systems: From CS-1 to XCS and its variants. *Evolutionary Intelligence*, 8(2–3):55–70.
- Bull, L. (2019). Autoencoding with a learning classifier system: Initial results. *arXiv*, 1907.11554.
- Bull, L. and Fogarty, T. C. (1994). Parallel evolution of communicating classifier systems. In *Proceedings of the First IEEE Conference on Evolutionary Computation*, volume 2, pages 680–685. Piscataway, NJ, USA: IEEE Press.
- Bull, L. and Hurst, J. (2003). A neural learning classifier system with self-adaptive constructivism. In Sarker, R. et al., editors, *Proceedings of the IEEE Congress on Evolutionary Computation*, volume 2, pages 991–997. Piscataway, NJ, USA: IEEE Press.
- Bull, L., Studley, M., Bagnall, A., and Whitley, I. (2007). Learning classifier system ensembles with rule-sharing. *IEEE Transactions on Evolutionary Computation*, 11(4):496–502.
- Butz, M. V. (2006). *Rule-Based Evolutionary Online Learning Systems*. Berlin, Germany: Springer-Verlag.
- Butz, M. V., Goldberg, D. E., and Lanzi, P.-L. (2005). Gradient descent methods in learning classifier systems: Improving XCS performance in multistep problems. *IEEE Transactions on Evolutionary Computation*, 9(5):452–473.
- Butz, M. V., Goldberg, D. E., and Tharakunnel, K. (2003). Analysis and improvement of fitness exploitation in XCS: Bounding models, tournament selection, and bilateral accuracy. *Evolutionary Computation*, 11(3):239–77.
- Butz, M. V., Kovacs, T., Lanzi, P.-L., and Wilson, S. W. (2004). Toward a theory of generalization and learning in XCS. *IEEE Transactions on Evolutionary Computation*, 8(1):28–46.
- Butz, M. V., Lanzi, P.-L., and Wilson, S. W. (2008). Function approximation with XCS: Hyperellipsoidal conditions, recursive least squares, and compaction. *IEEE Transactions on Evolutionary Computation*, 12(3):355–376.
- Casillas, J., Carse, B., and Bull, L. (2007). Fuzzy-XCS: A Michigan genetic fuzzy system. *IEEE Transactions on Fuzzy Systems*, 15(4):536–550.
- Cui, X., Zhang, W., Tüske, Z., and Picheny, M. (2018). Evolutionary stochastic gradient descent for optimization of deep neural networks. In Bengio, S. et al., editors, *Advances in Neural Information Processing Systems*, volume 31, pages 6051–6061. Red Hook, NY, USA: Curran Associates Inc.
- Dam, H. H., Abbass, H. A., Lokan, C., and Yao, X. (2008). Neural-based learning classifier systems. *IEEE Transactions on Knowledge and Data Engineering*, 20(1):26–39.
- Demšar, J. (2006). Statistical comparisons of classifiers over multiple data sets. *Journal of Machine Learning Research*, 7:1–30.
- Drugowitsch, J. and Barry, A. M. (2008). A formal framework and extensions for function approximation in learning classifier systems. *Machine Learning*, 70(1):45–88.



- Ebadi, T., Kukenys, I., Browne, W. N., and Zhang, M. (2014). Human-interpretable feature pattern classification system using learning classifier systems. *Evolutionary Computation*, 22(4):629–650.
- Erhan, D., Bengio, Y., Courville, A., Manzagol, P.-A., Vincent, P., and Bengio, S. (2010). Why does unsupervised pre-training help deep learning? *Journal of Machine Learning Research*, 11:625–660.
- Fernando, C., Banarse, D., Reynolds, M., Besse, F., Pfau, D., Jaderberg, M., Lanctot, M., and Wierstra, D. (2016). Convolution by evolution: Differentiable pattern producing networks. In Friedrich, T. et al., editors, *Proceedings of the Genetic and Evolutionary Computation Conference*, pages 109–116. New York, NY, USA: ACM.
- Gaier, A. and Ha, D. (2019). Weight agnostic neural networks. *arXiv*, 1906.04358.
- Gruau, F. and Whitley, D. (1993). Adding learning to the cellular development of neural networks: Evolution and the Baldwin effect. *Evolutionary Computation*, 1(3):213–233.
- He, K., Zhang, X., Ren, S., and Sun, J. (2015). Delving deep into rectifiers: Surpassing human-level performance on ImageNet classification. In Bajcsy, R., Hager, G., and Ma, Y., editors, *Proceedings of the IEEE International Conference on Computer Vision*, pages 1026–1034. Piscataway, NJ, USA: IEEE Press.
- Hinton, G. E. and Nowlan, S. J. (1987). How learning can guide evolution. *Complex Systems*, 1(3):495–502.
- Hinton, G. E. and Salakhutdinov, R. R. (2006). Reducing the dimensionality of data with neural networks. *Science*, 313(5786):504–507.
- Howard, D., Bull, L., and Lanzi, P.-L. (2016). A cognitive architecture based on a learning classifier system with spiking classifiers. *Neural Processing Letters*, 44(1):125–147.
- Iqbal, M., Browne, W. N., and Zhang, M. (2014). Reusing building blocks of extracted knowledge to solve complex, large-scale Boolean problems. *IEEE Transactions on Evolutionary Computation*, 18(4):465–480.
- Jaderberg, M., Dalibard, V., Osindero, S., Czarnecki, W. M., Donahue, J., Razavi, A., Vinyals, O., Green, T., Dunning, I., Simonyan, K., Fernando, C., and Kavukcuoglu, K. (2017). Population based training of neural networks. *arXiv*, 1711.09846.
- Khan, M. M., Ahmad, A. M., Khan, G. M., and Miller, J. F. (2013). Fast learning neural networks using Cartesian genetic programming. *Neurocomputing*, 121:274–289.
- Kim, J.-Y. and Cho, S.-B. (2019). Exploiting deep convolutional neural networks for a neural-based learning classifier system. *Neurocomputing*, 354:61–70.
- Lanzi, P.-L. and Loiacono, D. (2006). XCSF with neural prediction. In Yen, G. G. et al., editors, *Proceedings of the IEEE Congress on Evolutionary Computation*, pages 2270–2276. Piscataway, NJ, USA: IEEE Press.
- Lanzi, P.-L., Loiacono, D., and Zanini, M. (2008). Evolving classifier ensembles with voting predictors. In Michalewicz, Z. et al., editors, *Proceedings of the IEEE Congress on Evolutionary Computation*, pages 3760–3767. Piscataway, NJ, USA: IEEE Press.
- Lanzi, P.-L. and Wilson, S. W. (2006). Using convex hulls to represent classifier conditions. In Keijzer, M. et al., editors, *Proceedings of the Genetic and Evolutionary Computation Conference*, pages 1481–1488. New York, NY, USA: ACM.
- LeCun, Y., Bengio, Y., and Hinton, G. (2015). Deep learning. *Nature*, 521(7553):436–444.
- Loiacono, D., Marelli, A., and Lanzi, P.-L. (2007). Support vector regression for classifier prediction. In Thierens, D. et al., editors, *Proceedings of the Genetic and Evolutionary Computation Conference*, pages 1806–1813. New York, NY, USA: ACM.

- Matsumoto, K., Tatsumi, T., Sato, H., Kovacs, T., and Takadama, K. (2017). XCSR learning from compressed data acquired by deep neural network. *Journal of Advanced Computational Intelligence and Intelligent Informatics*, 21(5):856–867.
- Morse, G. and Stanley, K. O. (2016). Simple evolutionary optimization can rival stochastic gradient descent in neural networks. In Friedrich, T. et al., editors, *Proceedings of the Genetic and Evolutionary Computation Conference*, pages 477–484. New York, NY, USA: ACM.
- O’Hara, T. and Bull, L. (2005a). Building anticipations in an accuracy-based learning classifier system by use of an artificial neural network. In Corne, D. et al., editors, *Proceedings of the IEEE Congress on Evolutionary Computation*, volume 3, pages 2046–2052. Piscataway, NJ, USA: IEEE Press.
- O’Hara, T. and Bull, L. (2005b). A memetic accuracy-based neural learning classifier system. In Corne, D. et al., editors, *Proceedings of the IEEE Congress on Evolutionary Computation*, volume 3, pages 2040–2045. Piscataway, NJ, USA: IEEE Press.
- O’Hara, T. and Bull, L. (2007). Backpropagation in accuracy-based neural learning classifier systems. In Kovacs, T. et al., editors, *Learning Classifier Systems*, volume 4399 of *LNCS*, pages 25–39. Berlin, Germany: Springer-Verlag.
- Orriols-Puig, A., Bernadó-Mansilla, E., Goldberg, D. E., Sastry, K., and Lanzi, P.-L. (2009). Facetwise analysis of XCS for problems with class imbalances. *IEEE Transactions on Evolutionary Computation*, 13(5):1093–1119.
- Preen, R. J. and Bull, L. (2013). Dynamical genetic programming in XCSF. *Evolutionary Computation*, 21(3):361–387.
- Ranzato, M. A., Boureau, Y.-L., and LeCun, Y. (2007). Sparse feature learning for deep belief networks. In Platt, J. C. et al., editors, *Advances in Neural Information Processing Systems*, volume 20, pages 1185–1192. Red Hook, NY, USA: Curran Associates Inc.
- Rifai, S., Vincent, P., Muller, X., Glorot, X., and Bengio, Y. (2011). Contractive auto-encoders: Explicit invariance during feature extraction. In Ghahramani, Z., editor, *Proceedings of the International Conference on Machine Learning*, pages 833–840. Madison, WI, USA: Omnipress.
- Rumelhart, D. E., Hinton, G. E., and Williams, R. J. (1986). Learning representations by back-propagating errors. *Nature*, 323(6088):533–536.
- Sakurada, M. and Yairi, T. (2014). Anomaly detection using autoencoders with nonlinear dimensionality reduction. In Rahman, A., Deng, J. D., and Li, J., editors, *Proceedings of the MLSDA Workshop on Machine Learning for Sensory Data Analysis*, pages 4:4–4:11. New York, NY, USA: ACM.
- Sancho-Asensio, A., Orriols-Puig, A., and Golobardes, E. (2014). Robust on-line neural learning classifier system for data stream classification tasks. *Soft Computing*, 18(8):1441–1461.
- Schwefel, H.-P. (1981). *Numerical Optimization of Computer Models*. New York, NY, USA: John Wiley & Sons, Inc.
- Smith, R. E. and Cribbs, H. B. (1994). Is a learning classifier system a type of neural network? *Evolutionary Computation*, 2(1):19–36.
- Socher, R., Huang, E. H., Pennington, J., Ng, A. Y., and Manning, C. D. (2011). Dynamic pooling and unfolding recursive autoencoders for paraphrase detection. In Shawe-Taylor, J. et al., editors, *Advances in Neural Information Processing Systems*, volume 24. Red Hook, NY, USA: Curran Associates Inc.
- Srivastava, N., Hinton, G., Krizhevsky, A., Sutskever, I., and Salakhutdinov, R. (2014). Dropout: A simple way to prevent neural networks from overfitting. *Journal of Machine Learning Research*, 15:1929–1958.

- Stanley, K. O., Clune, J., Lehman, J., and Miikkulainen, R. (2019). Designing neural networks through neuroevolution. *Nature Machine Intelligence*, 1(1):24–35.
- Stanley, K. O., D’Ambrosio, D. B., and Gauci, J. (2009). A hypercube-based encoding for evolving large-scale neural networks. *Artificial Life*, 15(2):185–212.
- Stanley, K. O. and Miikkulainen, R. (2002). Evolving neural networks through augmenting topologies. *Evolutionary Computation*, 10(2):99–127.
- Stone, C. and Bull, L. (2003). For real! XCS with continuous-valued inputs. *Evolutionary Computation*, 11(3):299–336.
- Sun, Y., Yen, G. G., and Yi, Z. (2019). Evolving unsupervised deep neural networks for learning meaningful representations. *IEEE Transactions on Evolutionary Computation*, 23(1):89–103.
- Tamee, K., Bull, L., and Pinnigern, O. (2007). Towards clustering with XCS. In Thierens, D. et al., editors, *Proceedings of the Genetic and Evolutionary Computation Conference*, pages 1854–1860. New York, NY, USA: ACM.
- Turing, A. M. (1948). Intelligent machinery. In Evans, C. R. and Robertson, A. D. J., editors, *Cybernetics: Key Papers*. Baltimore, MD, USA and Manchester, UK: University Park Press. 1968.
- Vincent, P., Larochelle, H., Lajoie, I., Bengio, Y., and Manzagol, P. A. (2010). Stacked denoising autoencoders: Learning useful representations in a deep network with a local denoising criterion. *Journal of Machine Learning Research*, 11:3371–3408.
- Wan, L., Zeiler, M., Zhang, S., LeCun, Y., and Fergus, R. (2013). Regularization of neural networks using dropconnect. In Dasgupta, S. and McAllester, D., editors, *Proceedings of the International Conference on Machine Learning*, volume 28 of PMLR, pages 1058–1066. PMLR.
- Wilson, A. C., Roelofs, R., Stern, M., Srebro, N., and Recht, B. (2017). The marginal value of adaptive gradient methods in machine learning. In Guyon, I. et al., editors, *Advances in Neural Information Processing Systems*, volume 30, pages 4148–4158. Red Hook, NY, USA: Curran Associates Inc.
- Wilson, S. W. (1995). Classifier fitness based on accuracy. *Evolutionary Computation*, 3(2):149–175.
- Wilson, S. W. (2001). Function approximation with a classifier system. In Spector, L. et al., editors, *Proceedings of the Genetic and Evolutionary Computation Conference*, pages 974–981. San Francisco, CA, USA: Morgan Kaufmann.
- Wilson, S. W. (2002). Classifiers that approximate functions. *Natural Computing*, 1(2–3):211–234.
- Wyatt, D. and Bull, L. (2005). A memetic learning classifier system for describing continuous-valued problem spaces. In Hart, W. E., Smith, J. E., and Krasnogor, N., editors, *Recent Advances in Memetic Algorithms*, volume 166 of *STUDFUZZ*, pages 355–395. Berlin, Germany: Springer-Verlag.
- Xue, B., Zhang, M., Browne, W. N., and Yao, X. (2016). A survey on evolutionary computation approaches to feature selection. *IEEE Transactions on Evolutionary Computation*, 20(4):606–626.
- Yao, X. (1999). Evolving artificial neural networks. *Proceedings of the IEEE*, 87(9):1423–1447.
- Zeng, N., Zhang, H., Song, B., Liu, W., Li, Y., and Dobaie, A. M. (2018). Facial expression recognition via learning deep sparse autoencoders. *Neurocomputing*, 273:643–649.